Multiphysics topology optimization of aluminium and copper conductors for automotive electrical machines

Borja Lizarribar, Borja Prieto, Ahmed Selema (Member, IEEE), Mohamed N Ibrahim (Senior Member, IEEE), Peter Sergeant (Senior Member, IEEE), Gurutz Artetxe and Miguel Martínez-Iturralde

***Abstract*—This paper proposes loss & thermally optimised copper and aluminium structures for automotive electrical machines. A first batch of multiphysics optimisation is performed parametrically for 6 different electrical conductor topologies. Then, a multiphysics – thermal and electromagnetic – hybrid parametric and topology optimisation coupled with Multi Objective Differential Evolution (MODE) and with an additional step of Local Search (LS) is proposed. The introduced Topology Optimisation (TO) algorithm is explained in detail and applied to optimise electrical conductor geometries of pure Cu and AlSi10Mg. After that, the manufacturing by Additive Manufacturing (AM) of the most promising model is presented. The produced topology is benchmarked against a well-known fully rectangular structure. The proposed topology optimised geometry has been found to improve conventionally manufactured electrical conductors at intermediate frequencies, around 600-800 Hz, and improves considerably at high frequencies, achieving a reduction in losses of 58% at 2000 Hz comparing to a conventional rectangular copper structure.**

***Index Terms*—Electrical machines, optimization, Topology optimization, TO, Multiphysics optimization, Multiphysics TO, Thermal optimization, Electromagnetic optimization, Additive Manufacturing, AM, Copper AM, Aluminium AM, AlSi10Mg, Electrical conductors, AC losses reduction.**

I. Introduction

THE electrification of the automotive sector has grown exponentially in recent years [1]. As a result of this increased demand, various ways of improving the overall electric vehicle have been studied. One of these methods is to increase the shaft speed of the electric motor to improve the power density. However, the increase in shaft speed is accompanied by an increase in losses due to the high-frequency magnetic field, mainly in the stator lamination and the winding [2].

As for the high frequency losses in the electrical conductors, there are several methods of reducing them. For example, they can be mitigated by using a less electrically conductive material, such as AlSi10Mg [3]–[5], which can also improve the overall machine weight due to its reduced mass density. Other effective way of reducing AC winding losses is to control the position of the conductors within the slot [6], [7]. Conductors transposition is also a common method of reducing AC losses [8], [9]. Finally, a highly effective method of reducing high frequency losses in conductors is the use of Litz wire [10]–[12].

Despite the reduction in high frequency losses achieved by these methods, they normally affect negatively the losses at low frequency, for the lower copper slot fill factor or for the lower electrical conductivity of the material used.

While the automotive sector requires variable speed motors, it is necessary for said motors to have good performance at both low and high supply frequencies. In order to avoid the use of round conductors, which are known to have lower fill factor than flat conductors, the latest trend is to search for flat conductor geometries that are able to reduce AC losses without significantly decreasing the fill factor. In this context, a novel conductor shape is presented in [13] and compared with a purely rectangular shape. A geometry that follows the magnetic vector potential lines is presented in [14]. Another example of a shape to reduce AC losses can be found in [15]. The models presented in these 3 cases are hardly manufacturable using traditional production methods, but are easily fabricated using additive manufacturing (AM) approaches [16]–[19]. AM of electrical conductors opens the way to explore innovative topologies and new ways to reduce losses.

Regarding the freedom in manufacturable geometries offered by AM, Topology Optimisation (TO) has started to become an alternative to traditional parametric optimisation, due to the higher flexibility in exploring complex geometries and the better achieved performance.

TO is a widely used weight reduction method in mechanical design [20]–[22]. However, its application in the electromagnetics field is limited. Electromagnetic TO has mostly been applied to soft magnetic material parts, such as, rotors

B. Lizarribar (corresponding author: blizarribarc@ceit.es), B.Prieto, G. Artetxe and Miguel Martínez-Iturralde are with the Transport and Energy Division, CEIT-Basque Research and Technology Alliance (BRTA), Manuel Lardizabal 15, 20018 Donostia / San Sebastián, Spain. and also with the Universidad de Navarra, Tecnun, Manuel Lardizabal 13, 20018 Donostia / San Sebastián, Spain (e-mail: blizarribarc@ceit.es).

Ahmed Selema is with the Department of Electromechanical, Systems, and Metal Engineering, Ghent University, 9000 Ghent, Belgium, also with FlandersMake@UGent, Core Lab MIRO, 3001 Leuven, Belgium, and also with the Department of Electrical Engineering, Faculty of Engineering, Menoufia University, Menoufia 32511, Egypt.

Mohamed N. Ibrahim is with the Department of Electromechanical, Systems, and Metal Engineering, Ghent University, 9000 Ghent, Belgium, also with FlandersMake@UGent, Core Lab MIRO, 3001 Leuven, Belgium, and also with the Department of Electrical Engineering, Kafrelshiekh University, Kafrelshiekh 33511, Egypt.

Peter Sergeant is with the Department of Electromechanical, Systems, and Metal Engineering, Ghent University, 9000 Ghent, Belgium, and also with FlandersMake@UGent, Core Lab MIRO, 3001 Leuven, Belgium.

Manuscript received XXXXX, XXXXX; revised August XXXXXXX, XXXXXXX.

of synchronous reluctance [23]–[26] or permanent magnet motors [27]–[31]. The literature on TO of hard magnetic materials is scarce [32]–[34] and TO is rarely applied to electrical conductors. However, some examples of TO applied to electrical conductors can be found in the related literature. For example, in [35] TO is applied to conductors to achieve higher uniformity in the magnetic field in the region of interest for an electromagnet manipulator. Despite having applied the TO to conductors, it can be seen that the algorithm is applied for electromagnetic purposes only. Moreover, in [36] TO is applied to optimize the shape of an inductor coil. The objectives that are considered in this study are to achieve the most uniform temperature between 900-1300 ºC on a workpiece at a hardening depth of 1.2 mm and to maximize the power factor. The article presents a multiphysics TO - thermal and electromagnetic - but it focuses on an inductor coil operating at a fixed electrical frequency.

In this paper, a conductor geometry, difficult to produce using traditional methods and intended for an automotive application is presented and optimized via topological and parametric optimisation in terms of losses and machine temperature. A multiphysics - thermal & electromagnetic - hybrid parametric TO combined with Multi Objective Differential Evolution (MODE) [37] and a Local Search (LS) algorithm, is proposed, explained in detail and applied to an electrical conductor model. Thermal TO, let alone thermal-electromagnetic TO, has, to the authors' knowledge, never been considered in any study of TO of electrical machines. Moreover, the TO algorithm is applied to electrical conductor models with 2 different electrically conductive materials, pure Cu and AlSi10Mg. The most promising geometry obtained from the multiphysics TO is manufactured in AlSi10Mg by AM and it is benchmarked against a conventional copper and aluminium rectangular electrical conductor with even shapes for all the turns.

The presented article is arranged as follows. Firstly, the problem to be studied is shown, different conductor transposition possibilities are parametrically optimized and the best in terms of performance is selected in Section II. Afterwards, in Section III, the proposed TO algorithm is described and it is applied to one of the conductor transposition possibilities of pure copper. The introduced TO algorithm is used to optimise an electrical conductor geometry of AlSi10Mg in Section IV and a comparison between a copper and an aluminium rectangular electrical conductor and a topology optimised electrical conductor manufactured in AlSi10Mg by AM is shown in Section V. Finally, a brief summary and the conclusions derived from the work conducted are presented in Section VI.

II. Problem definition

The case study analysed in this article emulates two slots of a stator intended for an automotive application, having 8 hairpin conductors per slot and cooling via a casing water jacket placed in the outer part of the stator yoke. The problem is modelled in terms of 2D FEA in Altair Flux^{TM} and the simulation is defined as "*Steady-state AC magnetic coupled with Transient Thermal 2D*". This simulation consist on a coupled elecromagnetic-thermal simulation in which starting from a reference temperature, 20 ºC, the electromagnetic losses in the conductor are computed in steady-state AC and used to run a thermal transient model (losses in the stator iron are not considered in this study). The computed temperatures are used for the next simulation step. This calculation is repeated until the temperatures have stabilised.

A symmetry axis is defined in the FEA simulation in the y-axis, so that only one slot is modelled. This simplification, which has been proven equivalent to modelling a full two-slot model without symmetries, is considered so as to reduce computation time. The cooling is defined by a constant heat transfer coefficient in the line that would correspond to the outer diameter of the stator (see Fig. 1 (c)). The materials considered in the simulation model are:

- **M250-35A electrical steel**: for the stator lamination. Thermal conductivity of 47 W/m/K and heat capacity of 3900 kJ/m^3/K.
- **Copper**: with temperature dependent conductivity (electrical conductivity at 20 ºC, $\sigma_{20C} = 5.8 \cdot 10^7$ S $\cdot$ m). Thermal conductivity of 394 W/m/K and heat capacity of 3518 kJ/m^3/K.
- **Impregnation**: assumed to occupy all the space left inside the slot by the copper conductors. Thermal conductivity of 0.21 W/m/K and heat capacity of 396 kJ/m^3/K.

The simulation is performed with an input current of 25 A_{RMS} in the conductors, an initial temperature of 20 ºC, an ambient temperature of 20 ºC, a heat transfer coefficient for the cooling water jacket of 100 W/m^2/K and a water temperature of 20 ºC. Variable time-step is considered for the transient calculation having more steps at the simulation start.

Taking advantage of the fact that the resulting geometry is intended to be manufactured using AM methods, a similar approach to that presented in [38]–[40] is explored in this paper. The transposition of the conductors is done in the connection side to have as short end-windings as possible in the opposite side of the connection, as transposing the conductors leads to larger end-windings than those of regular coils.. In Fig. 1 a CAD model of the proposed method applied to the 4 turns closer to the airgap is shown. The figure illustrates how the 4th turn is divided in two when it steps to the 5th turn, and in upper turns the position of each one is transposed. Since the rotor field is not considered in the present case study, an adjacent two slot geometry can be considered equally representative of the behaviour of the magnetic fields and conductor losses in the automotive hairpin model mock-up.

Six different models are studied in detail using parametric optimisation. The models to be studied are the ones shown in Fig. 2; being, P1 the case in which all 8 conductors are solid, P2 the case in which 7 conductors are left solid and the conductor closer to the air gap is separated into 2 subconductors for transposition, P3 the case in which 6 conductors are solid and 2 transposed, and successively up to P6, in which just the bottom-most 3 conductors are left solid. No more configurations are considered as the limitation in conductor height and conductor separation does not permit

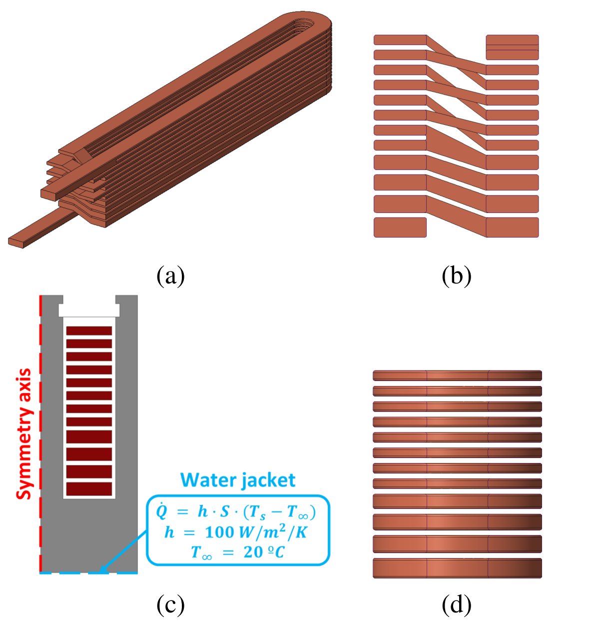

Fig. 1. Proposed model geometry for 4 solid and 4 tranposed conductors, (a) perspective view (b) front view - connection side (c) Altair Flux$^{\text{TM}}$ model (d) front view - non connection side.

to consider configurations with more subconductors which fit within the defined slot.

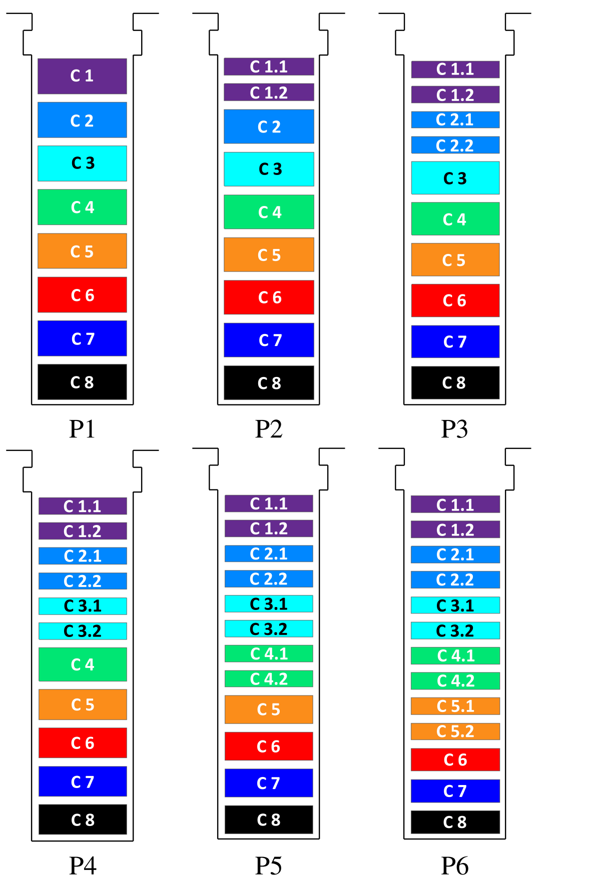

Fig. 2. Sketches of the models considered for the parametric optimization.

A parametric optimisation is performed on all the previously defined models. The parameters to be optimised are the height of each conductor, imposing a minimum height of 1 mm and a fixed conductor separation of 0.5 mm. The parametric optimisation is carried out using a Multi-Objective Differential Evolution (MODE) algorithm [37] and the output variables to be optimised are the maximum temperature at 1 Hz and the maximum temperature at 1 kHz, both of which are to be minimised. The results of the parametric optimisation are shown in Fig. 3, in terms of Pareto fronts for the maximum temperatures at nearly-DC and high frequency.

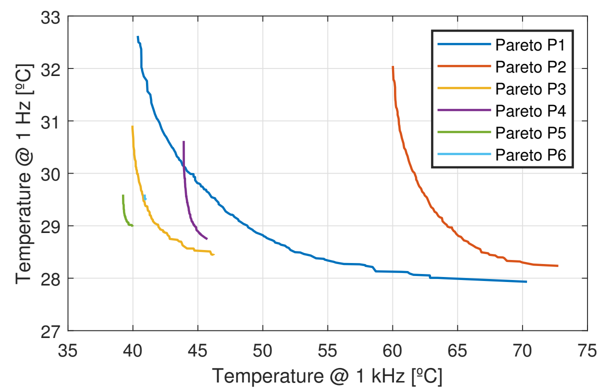

Fig. 3. Pareto fronts comparison between different models.

Several conclusions can be drawn from the parametric optimization results. The first one is that the most promising configuration to achieve a good balance between the two objectives is P5, the one with 4 solid turns and 4 divided into two and transposed. Despite the fact that P5 is the one that achieves the best results for the maximum temperature at high frequency (1 kHz), it is also seen that P1 is the one that has the best performance for maximum temperature at 1 Hz, as it was expected, since it leads to higher fill factor and, hence, lower DC resistance. It can also be seen that the Pareto front of P6 is narrow due to the limits imposed in terms of conductor height and conductor spacing. This means that this model cannot vary much from the original model in order to fit into the defined slot.

Although the electrical conductor model with the best performance is P5, TO is applied to P3 as it has more freedom of geometry variation due to the larger conductors that can fit into the slot with the defined geometric constraints.This geometric freedom is crucial to allow the TO algorithm to be able to remove any material from the conductor regions in order to try to improve the performance of the system.

III. MULTYPHYSICAL TO

After having defined the problem and once the most adequate model for TO, P3, has been selected, the proposed TO algorithm is discussed and applied in this section. For this case, the chosen TO approach is an on-off method, coupled with a normalised Gaussian network [41] method to speed up the simulation. The algorithm is considered a hybrid parametric-topology optimisation, as not only the distribution of the materials inside the defined region is optimised, but also the height of each conductor and subconductor are parametrically optmised along the simulation. A MODE [37] is used

This article has been accepted for publication in IEEE Transactions on Transportation Electrification. This is the author's version which has not been fully edited and content may change prior to final publication. Citation information: DOI 10.1109/TTE.2024.3367040

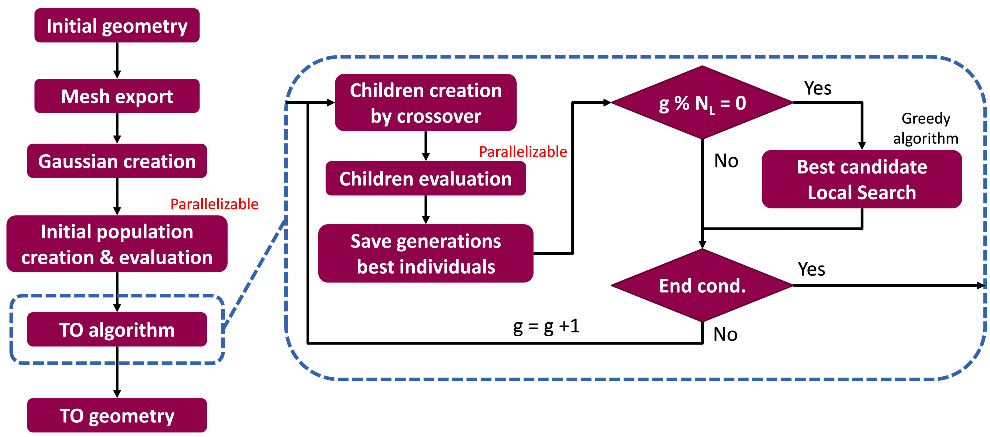

Fig. 4. Flowchart for the proposed TO algorithm.

as the underlying heuristic optimization algorithm and it is combined with a greedy local search algorithm [28] to favour the convergence of the method. This approach, ON-OFF + evolutionary, is known to be more time consuming than other TO methods, but as the problem to be analysed does not require a large computation time for each individual, around 30 seconds, the convergence speed is not the most critical aspect in this problem. Furthermore, this algorithm does not depend on gradients, which makes it easier to adapt to different objective functions. This is important in the case analysed, since the aim of this work is to carry out a multiphysics optimisation, taking into account electromagnetic and thermal aspects. Finally, it is harder for the algorithm used to get stuck in local optima, as is the case with other TO methods [42]. A flowchart representing the proposed TO method used is shown in Fig. 4.

The multiphysics hybrid parametric TO algorithm depicted in Fig. 4 works as follows. First, a geometry to be optimised is defined in the FEA program to be used for the calculation, Altair Flux$^{\text{TM}}$ in the presented case. The mesh is created in the FEA program and it is exported as data to Matlab®. The initial population is created and evaluated in the FEA program. The initial population is created randomly and the size of the first generation is of 800 individuals. After creating and evaluating the initial population, the TO algorithm starts. First, the next generation individuals, children, are created. Three of the most promising individuals from previous generation, parents, are combined by crossover and the defined number of children are created, in the case presented 100 for each generation. Additionally, randomly two of the parametric variables are changed. The children are evaluated and compared with parents. The best 100 individuals among the children and parents are selected to act as parents for the next generation. If the generation "g", is multiple of the defined number of generations to apply the Local Search "N_L", this algorithm is applied. The N_L defined for this case is of 30 generations. This procedure is repeated until an end condition is met, and the algorithm saves the results as Pareto fronts.

Finally, the objective that has been defined for the TO have been to minimise the maximum temperature at 1kHz and 1 Hz, as it has been defined for the parametric optimisations.

With the explained setup and calculating with 4 parallel computations, the TO algorithm needed of 4 days and 9 hours on a 12th Gen Intel® Core$^{\text{TM}}$ i5-12500 3.00 GHz, 6-cores, 16 GB RAM and a total of 19860 simulations. The results in terms of Pareto front are shown in Fig. 5. Also, the Altair Flux$^{\text{TM}}$ models for some of the most representative points of the Pareto front are represented in Fig. 5 and in Fig. 6.

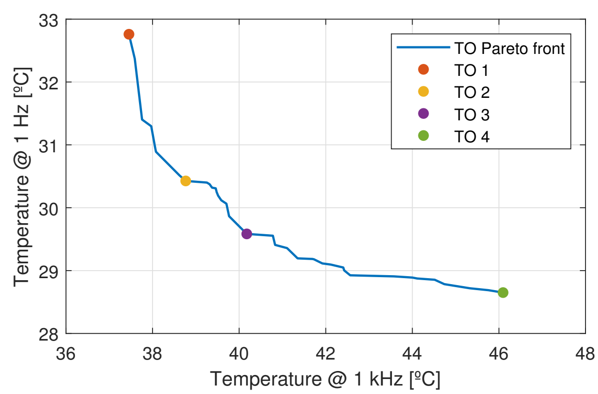

Fig. 5. Pareto front of the proposed TO algorithm.

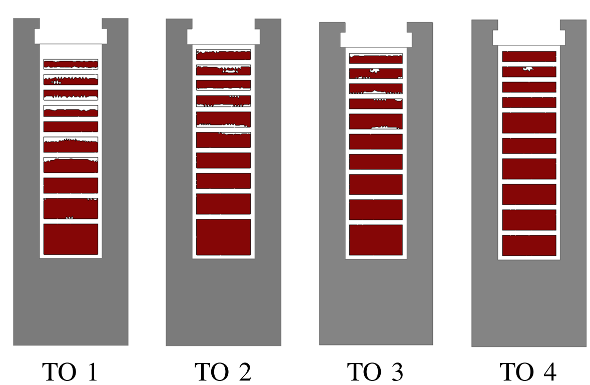

Fig. 6. Most representative individuals of TO.

It is noticeable from Fig. 6 that the resultant cross sections of the TO are in need of post-processing to smooth the sharp edges and to meet the requirements marked by the manufacturing method. The main one is that the minimum height manufacturable to ensure mechanical stability is 1 mm and that the distance between conductors must be larger or equal to 0.5 mm to ensure their correct insulation by employing 0.25 mm aramid paper tape. Although there are algorithms to perform this process automatically [43], in the present research work the smoothing has been done by hand.

Two different individuals, TO 1 and TO 2, have been selected from the Pareto front of the TO while they have the best performance at 1 kHz. The final geometric design for each of the two models is shown in Fig. 7. Table I summarises the main characteristics of each final model.

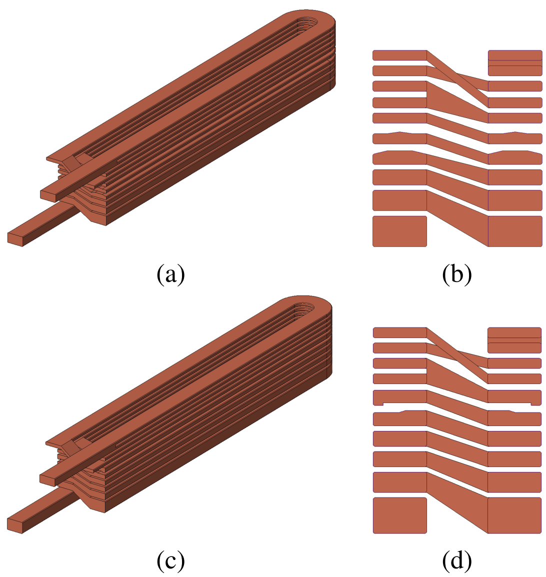

Fig. 7. TO 1 (a) perspective view, (b) front view and TO 2 (c) perspective view, (d) front view.

TABLE I
MAIN COMPARISON DATA BETWEEN MODELS.

	TO 1	TO 2
Temperature @ 1 kHz [ºC]	39.8 ºC	40.6 ºC
Temperature @ 1 Hz [ºC]	31.8 ºC	29.7 ºC
Losses @ 1 kHz [W]	1.57 W	1.66 W
Losses @ 1 Hz [W]	1.01 W	0.86 W
Weight [g]	175 g	159 g

Finally, as the differences found among models in Table I are small, a comparison of the losses obtained for different input frequencies at the two configurations with a purely rectangular configuration in which all conductors are equal (Fig. 8 (a)) and a Z-shape [44] (Fig. 8 (b)) is carried out in Fig. 9.

From Fig. 9 it can be seen how TO and conductors with non-conventional geometries can greatly improve the performance of an electrical machine at high frequencies compared

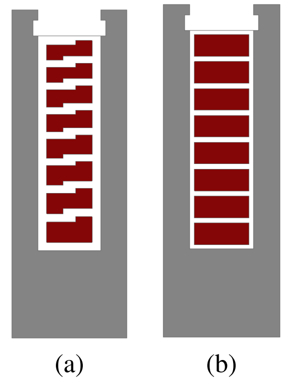

Fig. 8. (a) Z-shape proposed in [44] (b) Conventional rectangular electrical conductors

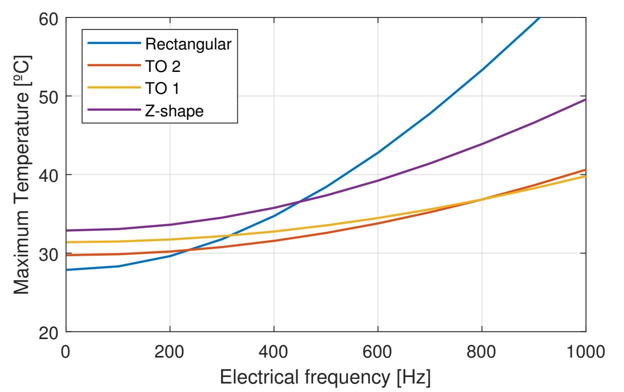

Fig. 9. Temperature comparison between models for different electrical current frequency.

to conventional rectangular ones ($\Delta T_{1kHz,rect} = 45.8°C$, $\Delta T_{1kHz,Z-Shape} = 29.6°C$, $\Delta T_{1kHz,TO1} = 19.8°C$).

IV. TO APPLIED TO ALSI10MG CONDUCTORS

AlSi10Mg, an aluminium-silicon-magnesium alloy, has great potential for electrical machine windings. This alloy offers a unique combination of properties that make it highly desirable for this application. Its low mass density enables the production of lightweight windings, contributing to the overall weight reduction of electrical machines. In addition, AlSi10Mg has excellent thermal conductivity, allowing efficient heat dissipation in high power applications. The electrical conductivity of AlSi10Mg can be significantly enhanced by appropriate post-treatments such as T6 heat treatment [44], [45]. The mechanical strength of this alloy can also be improved by stress relieving. Overall, AlSi10Mg offers a promising solution for electrical machine windings, providing a balance of favourable properties including reduced weight, efficient thermal management and improved electrical performance. Taking into account the presented advantages of AlSi10Mg in this section the previously explained algorithm is applied to the P3 model, but in this case defining the physical properties of AlSi10Mg instead of the pure Cu one.

In order to have a fair comparison between TO of pure Cu and AlSi10Mg electrical conductors, the optimisation objectives are modified to minimise the maximum temperature at

2.174 Hz and 2.174 kHz for the TO of AlSi10Mg conductors. This modification has been done in order the AlSi10Mg model to have the same skin depth as pure Cu at 1 Hz and 1 kHz. While skin depth is equal to $1/\sqrt{\pi f \mu \sigma}$, being "$f$" the electrical frequency, "μ" the magnetic permeability of the material and "σ" the electrical conductivity. Due to the different electrical conductivities of both materials to be analysed, AlSi10Mg (around 46 %IACS) and pure Cu (100 %IACS), the optimisation frequencies are changed to maintain the previously defined skin depth similar for both materials.

After applying the presented TO approach to AlSi10Mg electrical conductors, the candidate that achieves the best performance at high frequencies, AL 1, shown in Fig. 10 and Fig. 11, is selected from the Pareto front. Furthermore, a comparison between the TO candidates that minimises the temperature at high frequencies, TO 1 (best candidate for pure copper TO) and AL 1 (best candidate for AlSi10Mg TO), for different electrical frequencies is shown in Fig. 12.

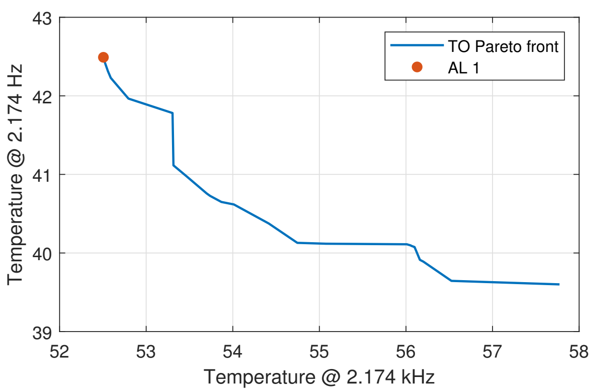

Fig. 10. Pareto front of the AlSi10Mg model.

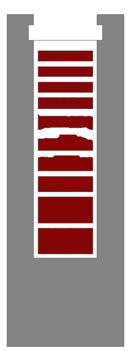

Fig. 11. AL 1 Altair Flux^{TM} electrical conductor model.

It can be extracted from Fig. 12 that as expected, AlSi10Mg geometry achieves higher maximum temperatures at low frequencies than pure Cu geometry, due to its lower electrical conductivity. However, for high frequency ranges, above 1900 Hz, the performance of AL 1 is better than TO 1 as AL 1 achieves lower maximum temperatures.

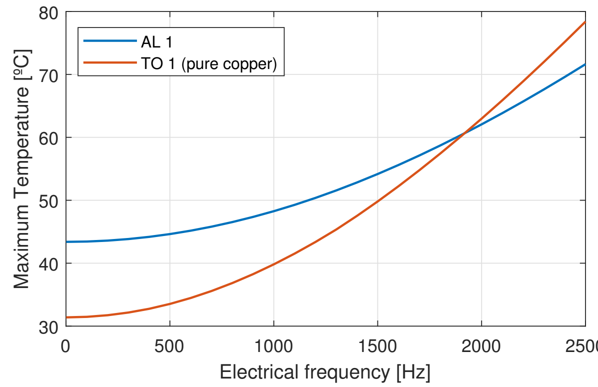

Fig. 12. Temperature comparison between AL 1 and TO 1 for different input electrical frequency.

V. Electrical conductor manufacturing & testing

This section presents the fabrication of the AL 1 geometry by AM of AlSi10Mg and a comparison with a traditional copper electrical conductor. The decision of producing AL 1 geometry in AlSi10Mg has been motivated by the low mass density of the material and its adequate electrical properties. In addition, the high cost of copper AM and the low electrical conductivity achieved in the manufacture of smaller testers has also been one of the reasons why copper has been discarded for the manufacture of the topology optimised geometry.

The aluminium prototype is printed by L-PBF in AlSi10Mg aluminium alloy. While the as-built mechanical and electrical properties are not good enough, a T6-heat treatment protocol [44], [45] is applied to the additively manufactured prototype.

In addition, the optimised geometry is compared to 2 conventional geometries with rectangular conductors of equal cross section in all turns, made of copper and aluminium. The main characteristics of the three models are summarised in Table II. The aluminium and copper geometries are shown in Fig. 13. This figure illustrates the produced prototypes assembled with the e-core where they have been tested to evaluate the AC losses. Due to the complexity of accurately measuring the maximum temperature, which is a very local phenomena, and while there is a strong relationship between losses and maximum temperature in this case, which can be deduced from Table I, the three geometries are compared in terms of losses for different input frequencies.

TABLE II
Measured properties and characteristics of tested prototypes.

	TO 1	**Conv. Cu**	**Conv. Al**
Material	AlSi10Mg	Cu	Al
Weight [g]	48.7 g	171.2 g	55.2 g
DC resistance [mΩ]	10.3 mΩ	3.9 mΩ	8.6 mΩ
Electrical conductivity [%IACS]	46 %IACS	100 %IACS	63 %IACS

To measure the losses at different input frequencies, the test bench in Fig. 14 has been employed. The main components

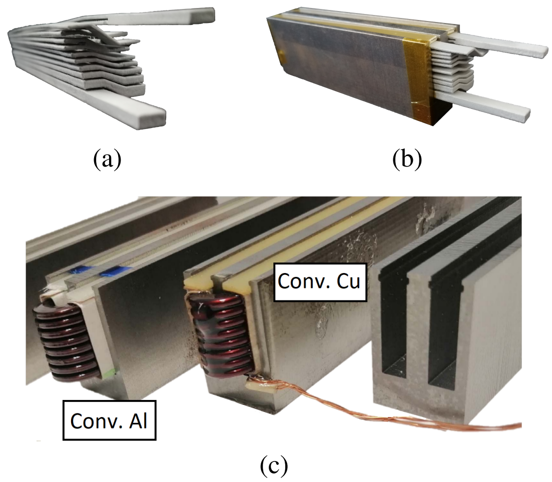

Fig. 13. Tested prototypes (a) AL 1 AM (b) AL 1 geometry assembled with the e-core and (c) copper (Conv. Cu) and aluminium (Conv. Al) conventional conductors assembled with the e-core.

of this test platform are an AC voltage and current source (Spitzenberger), voltage and current probes placed in the coil geometry, a data acquisition system (dSpace MicroLabBox) and a PA4000 (Tektronix) power analyser, used to measure AC and DC losses.

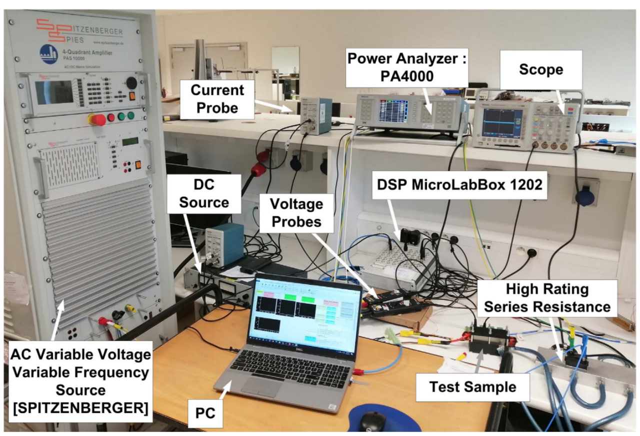

Fig. 14. Used test bench configuration to measure losses against frequency.

To have the most accurate results, temperature is controlled with a water jacket attached to the e-core maintaining a temperature of 25 °C and the samples are measured with an input current of 40 A_{RMS} for only 2 seconds, to avoid overheating the coil geometry. The results obtained for the three electrical conductor prototypes with an input current of 40 A_{RMS} and frequencies varying from 0 to 2000 Hz are shown in Fig. 15.

Several conclusions can be drawn from Table II and Fig. 15. First conclusion that can be extracted is that TO achieves a geometry that is able improve the performance of a conventional geometry from 600 Hz for aluminium and 800 Hz for copper. Additionally, a major improvement is seen at high frequencies, 2000 Hz, where AL 1 achieves a loss reduction of 58% with respect to copper conventional model and of 47% comparing to conventional aluminium model. On the other hand, due to the lower conductivity of AlSi10Mg and the lower slot fill factor of Al 1 the DC losses of this prototype are 2.6 times higher than the conventional rectangular copper geometry. Finally, taking into account that electrical conductors are one of the electrical machine components that contribute most to the total weight of the machine, Table II shows that the weight of the optimised geometry is only 28.4% of the conventional rectangular prototype. Regarding the comparison between tests and simulations, similar results have been obtained at low frequencies. However, for high frequencies, some discrepancies are observed. This could be due to inaccuracies when measuring the electrical conductivity of the test samples and local heating effects, both of which will affect the effective conductivity and the conductor losses. In any case, the trends between materials and geometries match and confirm the validity of the proposed optimization methodology.

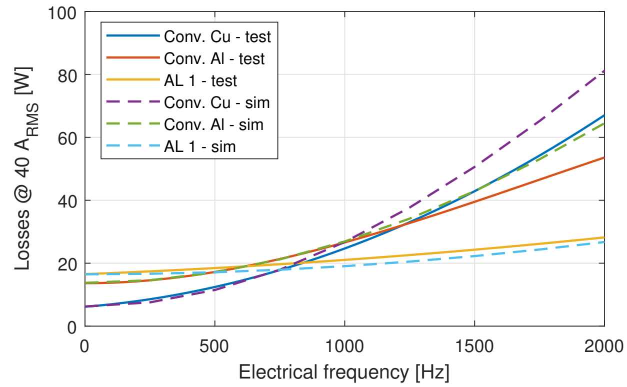

Fig. 15. Measured versus simulated losses for the tested geometries with an input current of 40 A_{RMS}.

VI. Conclusion

In this article a case study is presented involving a coil model manufactured by AM for automotive application. For maximizing the advantages of AM; mostly the freedom in manufacturable geometries, different models are presented and they are multiphysically optimized, electromagnetically and thermally, via parametric optimization. Additionally, the most promising conductor model is multiphysically topology optimised, considering two different materials, AlSi10Mg and pure Cu, with a proposed hybrid parametric TO algorithm, which can not be found in previous literature. The most promising geometry is additively manufactured in AlSi10Mg, tested and benchmarked against traditional rectangular copper and aluminium coil prototypes, showing a better performance at higher frequencies.

The importance of applying TO to refine the geometry and maximise the overall electrical machine performance has been highlighted in the work presented. This fact is clearly shown in Fig. 9, where a reduction in losses of 58% and 47% is achieved at 2000 Hz compared to conventional copper and aluminium prototypes, respectively.

As shortcomings of the present work, the main limitations are the following. To simplify the problem, the magnetic field of the rotor and iron losses on the stator have been neglected in this work. Both of these, will significantly impact the performance of any electrical machine and will likely affect the results obtained in terms of optimal conductor geometries. As future work, the addition of these two effects is contemplated. Additionally, it would be of great interest to analyse the effect of the cooling configuration in the TO results; that is the effect that having the heat sink closer to the heat source, as when dealing with hollow conductors or a slot-through configuration, has on the optimal geometries.

Finally, this study has developed a multiphysics topology optimisation method that is easily adaptable to different case studies and capable of significantly improving the thermal and loss performance of the conductors; always bearing in mind that TO approaches almost necessarily require AM techniques to produce the resulting complex shapes. This, in turn, owing to the high monetary costs of employing additive production methods, implies that the implementation of the proposed method should focus on high-end applications such as in automotive traction, high-frequency components and the aeronautical sector.

REFERENCES

[1] Why the automotive future is electric. https://www.mckinsey.com/industries/automotive-and-assembly/our-insights/why-the-automotive-future-is-electric#/. Accessed: 2023-03-06.

[2] Thomas A Lipo. *Introduction to AC Machine Design*. John Wiley & Sons, Inc., 8 2017.

[3] Hiroya Sugimoto, Yuto Yamada, and Kazuhito Imae. Analysis of winding ac loss in a permanent magnet synchronous machine with high slot fill aluminum winding. In *2022 International Power Electronics Conference (IPEC-Himeji 2022- ECCE Asia)*, pages 2741–2745, 2022.

[4] Ahmed Selema, Mohamed N. Ibrahim, and Peter Sergeant. Mitigation of high-frequency eddy current losses in hairpin winding machines. *Machines*, 10:328, 4 2022.

[5] Marco Pastura, Davide Barater, Stefano Nuzzo, and Giovanni Franceschini. Investigation of resistivity impact on ac losses in hairpin conductors. In *IECON 2021 – 47th Annual Conference of the IEEE Industrial Electronics Society*, pages 1–6, 2021.

[6] Anuvav Bardalai, David Gerada, Dmitry Golovanov, Zeyuan Xu, Xiaochen Zhang, Jing Li, He Zhang, and Chris Gerada. Reduction of winding ac losses by accurate conductor placement in high frequency electrical machines. *IEEE Transactions on Industry Applications*, 56(1):183–193, 2020.

[7] Ahmed Hebala, Stefano Nuzzo, Peter H. Connor, Giuseppe Volpe, Chris Gerada, and Michael Galea. Analysis and mitigation of ac losses in high performance propulsion motors. *Machines*, 10:780, 9 2022.

[8] Xinyue Chen, Haiyang Fang, Xinggang Fan, Haobo Hu, Dawei Li, and Ronghai Qu. Suppression of winding ac copper loss in high-speed electrical machines by a practical transposition technique. *IEEE Transactions on Industry Applications*, 58(6):7121–7130, 2022.

[9] Payam Shams Ghahfarokhi, Andrejs Podgornovs, Antonio J. Marques Cardoso, Ants Kallaste, Anouar Belahcen, and Toomas Vaimann. Hairpin windings for electric vehicle motors: Modeling and investigation of ac loss-mitigating approaches. *Machines*, 10:1029, 11 2022.

[10] Anuvav Bardalai, Xiaochen Zhang, Tianjie Zou, David Gerada, Jing Li, and Chris Gerada. Comparative analysis of ac losses with round magnet wire and litz wire winding of a high – speed pm machine. In *2019 22nd International Conference on Electrical Machines and Systems (ICEMS)*, pages 1–5, 2019.

[11] Maria Sofia C. Pechlivanidou and Antonios G. Kladas. Litz wire strand shape impact analysis on ac losses of high-speed permanent magnet synchronous motors. In *2021 IEEE Workshop on Electrical Machines Design, Control and Diagnosis (WEMDCD)*, pages 95–100, 2021.

[12] Henry Hamalainen, Juha Pyrhonen, Janne Nerg, and Joonas Talvitie. Ac resistance factor of litz-wire windings used in low-voltage high-power generators. *IEEE Transactions on Industrial Electronics*, 61:693–700, 2 2014.

[13] Ahmed Selema, Mohamed N. Ibrahim, and Peter Sergeant. Additively-manufactured ultra-light shaped-profile windings for hf electrical machines and weight-sensitive applications. *IEEE Transactions on Transportation Electrification*, pages 1–1, 2022.

[14] Nick Simpson, Dominic J. North, Suzanne M. Collins, and Phil H. Mellor. Additive manufacturing of shaped profile windings for minimal ac loss in electrical machines. *IEEE Transactions on Industry Applications*, 56:2510–2519, 5 2020.

[15] R. Notari, M. Pastura, S. Nuzzo, D. Barater, G. Franceschini, and C. Gerada. Ac losses reduction in hairpin windings produced via additive manufacturing. In *2022 International Conference on Electrical Machines (ICEM)*, pages 1144–1149. IEEE, 9 2022.

[16] Xiaotao Ren, Adrien Thabuis, and Yves Perriard. Innovative design of 3d-printed winding for linear motor. In *2022 25th International Conference on Electrical Machines and Systems (ICEMS)*, pages 1–6, 2022.

[17] Fan Wu, Ayman M. EL-Refaie, and Ali Al-Qarni. Minimization of winding ac losses using inhomogeneous electrical conductivity enabled by additive manufacturing. *IEEE Transactions on Industry Applications*, 58:3447–3458, 5 2022.

[18] C. Wohlers, P. Juris, S. Kabelac, and B. Ponick. Design and direct liquid cooling of tooth-coil windings. *Electrical Engineering*, 100:2299–2308, 12 2018.

[19] F. Lorenz, J. Rudolph, and Ralf Wemer. Design of 3d printed high performance windings for switched reluctance machines. In *2018 XIII International Conference on Electrical Machines (ICEM)*, pages 2451–2457, 2018.

[20] Mafalda Gonçalves, A. Andrade-Campos, and Bruno Barroqueiro. On the design of mechanical heterogeneous specimens using multilevel topology optimization. *Advances in Engineering Software*, 175:103314, 01 2023.

[21] Xiaoyan Teng, Can Wang, Xudong Jiang, and Xiangyang Chen. Structural topology optimization with local finite-life fatigue constraints. *Mathematics*, 11:1220, 3 2023.

[22] Chih-Hsing Liu, Yang Chen, and Sy-Yeu Yang. Topology optimization and prototype of a multimaterial-like compliant finger by varying the infill density in 3d printing. *Soft Robotics*, 9:837–849, 10 2022.

[23] Changwoo Lee, Jaewook Lee, and In Gwun Jang. Topology optimization for the manufacturable and structurally safe synchronous reluctance motors with multiple iron webs and bridges. *IEEE Transactions on Industrial Electronics*, 70:678–687, 1 2023.

[24] Feng Guo and Ian P. Brown. Simultaneous magnetic and structural topology optimization of synchronous reluctance machine rotors. *IEEE Transactions on Magnetics*, 56:1–12, 10 2020.

[25] Yu Li, Bo Ma, Jing Zheng, Jianguo Zhu, and Gang Lei. Electromagnetic and mechanical topology optimization for synrm rotors considering high dimensional constraints. *IEEE Transactions on Industrial Electronics*, pages 1–12, 2023.

[26] Oğuz Korman, Mauro Di Nardo, Michele Degano, and Chris Gerada. On the use of topology optimization for synchronous reluctance machines design. *Energies*, 15:3719, 5 2022.

[27] Takeo Ishikawa, Peijie Xie, and Nobuyuki Kurita. Topology optimization of rotor structure in permanent magnet synchronous motors considering ease of manufacturing. *IEEJ Journal of Industry Applications*, 4:469–475, 2015.

[28] Takahiro Sato, Kota Watanabe, and Hajime Igarashi. Multimaterial topology optimization of electric machines based on normalized gaussian network. *IEEE Transactions on Magnetics*, 51:1–4, 3 2015.

[29] Gyeong Uk Jang, Seunghyeon Cho, Jaemin Moon, Kyunghun Jeon, and Chang wan Kim. Topology optimization to reduce electromagnetic force induced vibration for the specific frequency of pmsm motor using electromagnetic-structural coupled analysis. *Energies*, 14:431, 1 2021.

[30] Changwoo Lee and In Gwun Jang. Topology optimization of the ipmsms considering both the mtpa and fw controls under the voltage and current limitations. *IEEE Transactions on Industrial Electronics*, pages 1–9, 2023.

[31] Changwoo Lee and In Gwun Jang. Multi-material topology optimization for the pmsms under the consideration of the mtpa control. *Structural and Multidisciplinary Optimization*, 65:263, 9 2022.

[32] Jiawei Tian, Ran Zhuang, Juan Cilia, Arvind Rangarajan, Fang Luo, Jon Longtin, and Shikui Chen. Topology optimization of permanent magnets for generators using level set methods. In *Volume 3B: 48th Design Automation Conference (DAC)*. American Society of Mechanical Engineers, 8 2022.

[33] Jaejoon Lee, Jaewook Lee, Taehoon Jung, and Jeonghoon Yoo. Topology optimization for three-dimensional design of segmented permanent

magnet arrays. *Structural and Multidisciplinary Optimization*, 62:3089–3104, 12 2020.

[34] R. Bjørk, C.R.H. Bahl, and A.R. Insinga. Topology optimized permanent magnet systems. *Journal of Magnetism and Magnetic Materials*, 437:78–85, 2017.

[35] Adrien Thabuis, Maribel Caceres Rivera, Xiaotao Ren, and Yves Perriard. Topology optimization of an electromagnet manipulator for 3d uniform magnetic field generation. *IEEE Transactions on Magnetics*, pages 1–1, 2023.

[36] Jmag: Optimizations solutions - topology optimization. https://www.youtube.com/watch?v=eQL9Mg0BHmg. Accessed: 2023-03-10.

[37] Rainer Storn and Kenneth Price. Differential Evolution-A Simple and Efficient Heuristic for Global Optimization over Continuous Spaces. Technical report, 1997.

[38] Ahmed Selema, Mohamed N. Ibrahim, and Peter Sergeant. Development of novel semi-stranded windings for high speed electrical machines enabled by additive manufacturing. *Applied Sciences*, 13:1653, 1 2023.

[39] Marco Pastura, Riccardo Notari, Stefano Nuzzo, Davide Barater, and Giovanni Franceschini. Ac losses analysis and design guidelines for hairpin windings with segmented conductors. *IEEE Transactions on Transportation Electrification*, pages 1–1, 2023.

[40] Nick Simpson, Jakob Jung, Axel Helm, and Phil Mellor. Additive manufacturing of a conformal hybrid-strand concentrated winding topology for minimal ac loss in electrical machines. pages 3844–3851. IEEE, 10 2021.

[41] Shunpei Sato, Takahiro Sato, and Hajime Igarashi. Topology optimization of synchronous reluctance motor using normalized gaussian network. *IEEE Transactions on Magnetics*, 51(3):1–4, 2015.

[42] FNU Nishanth and Bingnan Wang. Topology optimization of electric machines: A review. In *2022 IEEE Energy Conversion Congress and Exposition (ECCE)*, pages 1–8, 2022.

[43] Yutaka Ohtake, Alexander G. Belyaev, and Ilia A. Bogaevski. Polyhedral surface smoothing with simultaneous mesh regularization. *Proceedings Geometric Modeling and Processing 2000. Theory and Applications*, pages 229–237, 2000.

[44] Ahmed Selema, Mohamed N. Ibrahim, and Peter Sergeant. Additively manufactured ultralight shaped-profile windings for hf electrical machines and weight-sensitive applications. *IEEE Transactions on Transportation Electrification*, 8(4):4313–4324, 2022.

[45] Cassidy Silbernagel, Ian Ashcroft, Phill Dickens, and Michael Galea. Electrical resistivity of additively manufactured alsi10mg for use in electric motors. *Additive Manufacturing*, 21:395–403, 2018.